AMERICAN SOCIETY FOR MICROBIOLOGY | Journal of Virology®

VIRUS-CELL INTERACTIONS

Schlafen 11 Restricts Flavivirus Replication

Federico Valdez,[a] Julienne Salvador,[a] Pedro M. Palermo,[a] Jonathon E. Mohl,[b] Kathryn A. Hanley,[c] Douglas Watts,[a] Manuel Llano[a]

[a]Department of Biological Sciences, The University of Texas at El Paso, El Paso, Texas, USA
[b]Department of Bioinformatics, The University of Texas at El Paso, El Paso, Texas, USA
[c]Department of Biology, New Mexico State University, Las Cruces, New Mexico, USA

ABSTRACT Schlafen 11 (Slfn11) is an interferon-stimulated gene that controls the synthesis of proteins by regulating tRNA abundance. Likely through this mechanism, Slfn11 has previously been shown to impair human immunodeficiency virus type 1 (HIV-1) infection and the expression of codon-biased open reading frames. Because replication of positive-sense single-stranded RNA [(+)ssRNA] viruses requires the immediate translation of the incoming viral genome, whereas negative-sense single-stranded RNA [(−)ssRNA] viruses carry at infection an RNA replicase that makes multiple translation-competent copies of the incoming viral genome, we reasoned that (+)ssRNA viruses will be more sensitive to the effect of Slfn11 on protein synthesis than (−)ssRNA viruses. To evaluate this hypothesis, we tested the effects of Slfn11 on the replication of a panel of ssRNA viruses in the human glioblastoma cell line A172, which naturally expresses Slfn11. Depletion of Slfn11 significantly increased the replication of (+)ssRNA viruses from the *Flavivirus* genus, including West Nile virus (WNV), dengue virus (DENV), and Zika virus (ZIKV), but had no significant effect on the replication of the (−)ssRNA viruses vesicular stomatitis virus (VSV) (*Rhabdoviridae* family) and Rift Valley fever virus (RVFV) (*Phenuiviridae* family). Quantification of the ratio of genome-containing viral particles to PFU indicated that Slfn11 impairs WNV infectivity. Intriguingly, Slfn11 prevented WNV-induced downregulation of a subset of tRNAs implicated in the translation of 11.8% of the viral polyprotein. Low-abundance tRNAs might promote optimal protein folding and enhance viral infectivity, as previously reported. In summary, this study demonstrates that Slfn11 restricts flavivirus replication by impairing viral infectivity.

IMPORTANCE We provide evidence that the cellular protein Schlafen 11 (Slfn11) impairs replication of flaviviruses, including West Nile virus (WNV), dengue virus (DENV), and Zika virus (ZIKV). However, replication of single-stranded negative RNA viruses was not affected. Specifically, Slfn11 decreases the infectivity of WNV potentially by preventing virus-induced modifications of the host tRNA repertoire that could lead to enhanced viral protein folding. Furthermore, we demonstrate that Slfn11 is not the limiting factor of this novel broad antiviral pathway.

KEYWORDS Schlafen 11, virus restriction factors, flavivirus

Successful viral replication depends on the ability of the virus to appropriate the host translational machinery. The innate immune response exploits this dependency to control viral replication. Many interferon (IFN)-stimulated genes (ISGs) that regulate protein translation are well known to restrict virus replication, including protein kinase R, the interferon-induced proteins with tetratricopeptide repeats family of proteins, zinc finger antiviral protein, and the 2′,5′-oligoadenylate/RNase L pathway. The Schlafen (Slfn) proteins, another family of ISGs, were first identified as being important regulators of T cell differentiation and growth (1, 2). Currently, 10 mouse (Slfn1, -1L, -2, -3, -4, -5, -8, -9, -10, and -14) and 6 human (Slfn5, -11, -12, -12L, -13, and -14) Slfn genes have been

Citation Valdez F, Salvador J, Palermo PM, Mohl JE, Hanley KA, Watts D, Llano M. 2019. Schlafen 11 restricts flavivirus replication. J Virol 93:e00104-19. https://doi.org/10.1128/JVI.00104-19.

Editor Mark T. Heise, University of North Carolina at Chapel Hill

Address correspondence to Manuel Llano, mllano@utep.edu.

Received 22 January 2019
Accepted 14 May 2019
Accepted manuscript posted online 22 May 2019
Published 17 July 2019

identified (1, 2). Slfn11, the focus of the present study, is ubiquitously expressed in human tissues (3) but is absent in mice (1, 2). This protein controls the synthesis of proteins encoded by codon-biased open reading frames (3–5).

Several members of the Schlafen family have been shown to impair virus replication. Mouse Slfn14 impairs replication of influenza A and varicella zoster virus. The mechanism for this effect is unknown, but Slfn14 affects nuclear trafficking of influenza nucleoproteins and enhances IFN-β signaling (6). Human Slfn11 suppresses human immunodeficiency virus type 1 (HIV-1) and equine infectious anemia virus infection (4, 5). Slfn11 binds to tRNAs and counteracts the upregulation of the tRNA repertoire induced by HIV-1 infection that promotes translation of the codon-biased viral genome (4). The antiviral mechanism of Slfn11 seems to involve a tRNA nucleolytic activity recently described for Slfn13 (7). Eight out of nine residues implicated in the tRNA nucleolytic activity of Slfn13 (7) are conserved in Slfn11, and these two proteins share an overall homology of 83%. This enzymatic activity is required for Slfn13 to restrict HIV-1 infection. Slfn13 cleaves tRNAs close to the 3′ end at the acceptor stem and also diminishes the levels of HIV-1 mRNA. The anti-HIV-1 activity of Slf13 is specific since this protein did not affect replication of herpes simplex virus or Zika virus (ZIKV) (7).

Considering the effect of Slfn11 on protein synthesis, we hypothesized that this protein would preferentially restrict the replication of positive-sense single-stranded RNA [(+)ssRNA] viruses over negative-sense ssRNA [(−)ssRNA] viruses. Replication of (+)ssRNA viruses requires the immediate translation of the incoming viral genome. In contrast, (−)ssRNA viruses do not have this dependency, as they introduce upon infection an RNA-dependent RNA polymerase that uses the incoming viral genome as the template to produce multiple copies of translation-competent viral RNA. Therefore, (+)ssRNA viruses are expected to be more sensitive to impaired protein translation than (−)ssRNA viruses, as recently evidenced (8).

Based on this, we predicted that knockdown (KD) of Slfn11 would enhance the replication of (+)ssRNA viruses but have no effect on the replication of (−)ssRNA viruses. Consequently, we predicted that overexpression of Slfn11 would restrict the replication of (+)ssRNA but not (−)ssRNA viruses. Finally, we expected to see that West Nile virus (WNV) infection would modulate the tRNA repertoire in Slfn11-deficient cells but not in cells expressing this protein. We tested these predictions and found that flaviviruses, including WNV, dengue virus (DENV), and ZIKV, replicated significantly more efficiently in Slfn11-deficient than in control cells expressing this protein. However, this phenotype was not observed when the replication of the (−)ssRNA viruses vesicular stomatitis virus (VSV) (*Rhabdoviridae* family) and Rift Valley fever virus (RVFV) (*Phenuiviridae* family) was analyzed, highlighting the specificity of this antiviral activity. Furthermore, quantification of the ratio of genome-containing viral particles to PFU in the supernatant of infected cells demonstrated that Slfn11 impairs WNV infectivity. Analysis of the tRNA repertoire indicated that Slfn11 prevented the WNV-induced downregulation of the expression of a subset of tRNAs implicated in the translation of the viral polyprotein. Finally, we found that cells lacking endogenous Slfn11 failed to support the antiviral activity of exogenously introduced Slfn11. In summary, our data demonstrate that Slfn11 decreases viral infectivity, restricting the replication of flaviviruses.

(This article was submitted to an online preprint archive [9].)

RESULTS

WNV infection induces expression of Slfn11. To determine whether WNV infection modulates levels of Slfn11 expression, we characterized cells of the human glioblastoma cell line A172. These cells were demonstrated to be highly susceptible to WNV infection and to modulate the expression of a subset of genes implicated in neurodegeneration (10). To further verify the suitability of this cellular model for WNV replication, we compared the susceptibilities of Vero and A172 cells to WNV. Cells were infected at a multiplicity of infection (MOI) of 1, and the level of WNV envelope protein (E) was determined by flow cytometry analysis with a specific antibody. Results from

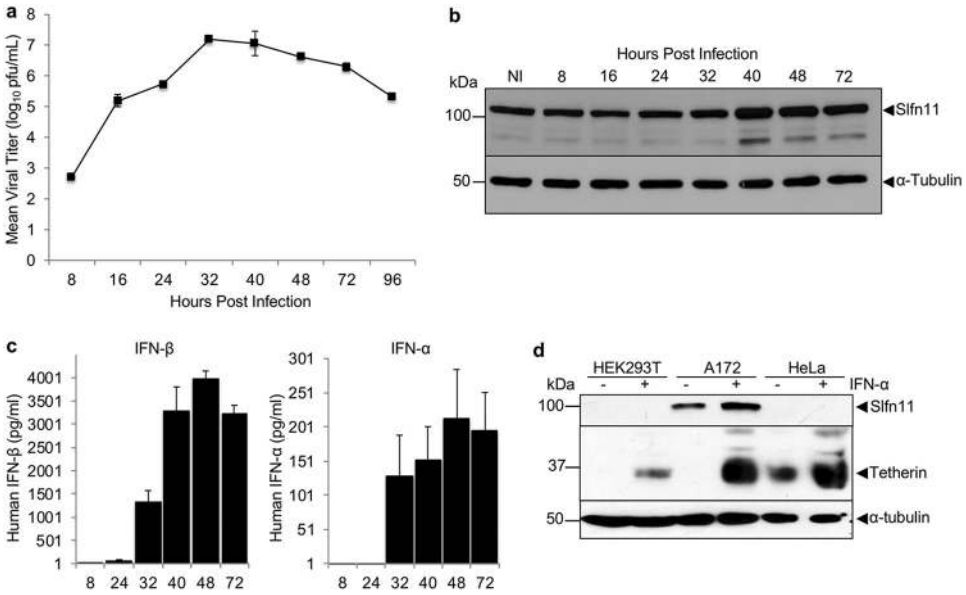

FIG 1 Kinetics of WNV replication, type I interferon production, and Slfn11 expression in A172 cells. (a) WNV replication in A172 cells. Cells were infected with WNV at an MOI of 0.1, and viral replication was measured by titration of the cell supernatant in a plaque assay at different times postinfection. Titers were determined in triplicate experiments. Data represent the means ± standard errors of the means from three independent experiments. The *x* axis is not to scale. NI, not infected. (b) Expression of Slfn11 in WNV-infected A172 cells. Cells were lysed at different times postinfection, and Slfn11 and α-tubulin (loading control) were detected with specific antibodies by immunoblotting. Results are representative of data from 2 independent infection experiments. (c) Kinetics of IFN-α and IFN-β (all subtypes) production in WNV-infected A172 cells. The culture supernatant was collected at different times postinfection, and type I IFN was quantified by an ELISA. Data represent the means ± standard errors of the means from three independent experiments. (d). Effect of IFN-α1 on Slfn11 expression. HeLa, A172, and HEK293T cells were treated with 5,000 U/ml of IFN-α1 for 24 h, and the expression levels of the type I IFN-stimulated genes Slfn11 and tetherin were evaluated by immunoblotting.

two independent infection experiments indicated that A172 cells were as susceptible as Vero cells to WNV infection. At 12 h postinfection (p.i.), 11% ± 0.22% of A172 cells and 15% ± 0.85% of Vero cells expressed WNV E protein, and 100% of the cells of both cell lines were positive for this structural viral protein at 32 h postinfection.

A172 cells were infected with WNV at an MOI of 0.1, and viral replication and expression of Slfn11 were determined at different times p.i. by a plaque assay and immunoblotting, respectively (Fig. 1a and b). Viral replication was detectable by as early as 8 h p.i. and peaked by 32 h after infection (Fig. 1a). Corresponding with the peak of viral replication, we detected a sustained increase in the basal levels of Slfn11 after 40 h p.i. (Fig. 1b). Densitometry analysis of immunoblots from two independent infection experiments indicated that WNV infection caused a 3.5-fold increase in the α-tubulin-normalized Slfn11 protein levels after 40 h p.i. Therefore, these data indicated that Slfn11 is upregulated by WNV infection.

Taking into consideration the role of type I IFN in the expression of Slfn11, the upregulation of Slfn11 in WNV-infected cells could be secondary to the production of this cytokine in response to viral infection. Therefore, we evaluated the temporal sequence of the production of these proteins. A172 cells were infected with WNV, as described above, and levels of IFN-α and -β were determined in the cell supernatant by an enzyme-linked immunosorbent assay (ELISA). IFN-α and -β were undetectable, at <1.95 pg/ml and <2.3pg/ml, respectively, at 8 h p.i., even though viral replication was evident by this time (Fig. 1c). However, type I IFN production was evident by 32 h, reaching a peak 48 h after infection. Therefore, these data indicated a temporal correspondence between type I IFN secretion and the upregulation of Slfn11, suggesting that virus-induced type I IFN upregulated Slfn11 expression.

To further evaluate the role of type I IFN in the regulation of Slfn11 expression, a panel of cell lines susceptible to WNV infection was treated with IFN-α1 for 24 h, and

the levels of Slfn11 were then determined by immunoblotting. Similar to WNV infection, IFN-α1 triggered a 2-fold increase in the level of Slfn11 in A172 cells (Fig. 1d). However, this treatment failed to induce the expression of Slfn11 in HEK293T or HeLa cells, which also lack basal expression of this protein. To verify that IFN-α1 stimulated these cells, we also measured the expression of the ISG tetherin. As previously reported, tetherin was constitutively expressed in HeLa cells but not in HEK293T cells, and the expression of this protein was increased in both cell types in response to IFN-α1 stimulation (Fig. 1d). Tetherin was absent in untreated A172 cells but was also significantly induced after IFN-α1 treatment. Therefore, the lack of a response to IFN-α1 was not the reason for the absence of Slfn11 in HeLa and HEK293T cells.

Slfn11 impairs replication of flaviviruses but not of (−)ssRNA viruses. To test the relative effect of Slfn11 expression on (+)ssRNA and (−)ssRNA viruses, A172 cells were stably transduced with lentiviral vectors expressing short hairpin RNAs (shRNAs) containing Slfn11-specific (4) or scrambled (SCR) sequences to generate Slfn11-deficient A172 cells (A172-KD) and control cells (A172-SCR), respectively. Subsequently, A172-KD cells were engineered to overexpress Slfn11 (A172-BC). Levels of Slfn11 were verified in these cells by immunoblotting (Fig. 2a). Next, A172-derived cell lines were infected with WNV at MOIs of 0.1 and 1, and cell culture supernatants were collected every 8 h to measure viral titers by a plaque assay.

For all the replication curves reported in this study, we analyzed the data with repeated-measures analysis of variance (ANOVA) and a Tukey-Kramer *post hoc* test. As shown in Fig. 2b and c, there was a significant interaction of the effects of cell type (A172-KD, -SCR, or -BC) and time p.i. on WNV titer (df = 14, $F = 11.1$, and $P < 0.0001$). Overall, WNV replicated significantly more efficiently in A172 cells lacking Slfn11 than in either of the two cell lines expressing this protein (Fig. 2b and c). Importantly, reexpression of Slfn11 in KD cells removed the enhanced permissiveness of these cells to viral infection. At an MOI of 0.1, at 24 h postinfection, viral titers were 2 logs higher in Slfn11-deficient cells than in control cells, and these differences persisted until 96 h postinfection (Fig. 2b). Similarly, at an MOI of 1, viral titers were 1 log higher in Slfn11 knockdown cells than in control cells, and these differences were observed from 24 to 48 h postinfection (Fig. 2c). At both MOIs, no differences in cytopathic effects were observed between the cell lines evaluated; the cytopathic effects were more noticeable after 48 h postinfection and led to termination of the experiments 96 h after infection.

We anticipated that Slfn11 would impair WNV replication by targeting viral protein production. Therefore, we infected A172-derived cells with WNV at an MOI of 0.1 and measured cell-associated WNV envelope (E) protein at the peak of infection (40 h p.i.) by immunoblot analysis. As expected, Slfn11-deficient cells expressed higher levels of WNV E than did control cells (Fig. 2d). Densitometry analysis of the immunoblots corresponding to three independent infection experiments indicated that α-tubulin-normalized E levels were similar between A172-SCR and -BC cells, and A172-KD cells expressed 12.3-fold more E protein than A172-SCR cells. These results were expected based on the WNV titer reached in these cells and on the postulated mechanism of action of Slfn11.

In addition, we verified WNV E expression by indirect immunofluorescence. A172-derived cell lines were infected with WNV at an MOI of 1, and the production of WNV E was evaluated 24 and 48 h after infection by indirect immunofluorescence with an antiflavivirus antibody that reacts with WNV E. In correspondence with data in Fig. 2d, Slfn11-deficient cells expressed higher levels of E than did A172-SCR and -BC cells at 48 h p.i. (Fig. 2e). As expected, analysis at 24 h postinfection showed similar results (data not shown). Therefore, data in Fig. 2b to e demonstrated that Slfn11 markedly impaired the replication of WNV by impairing viral protein expression.

We next tested whether Slfn11 affected the replication of two additional flaviviruses, DENV and ZIKV. Contrary to WNV, DENV does not replicate efficiently in A172 cells; however, we were interested in determining the contribution of Slfn11 to this phenotype. Thus, A172-derived cells were infected with DENV at an MOI of 0.1, and viral

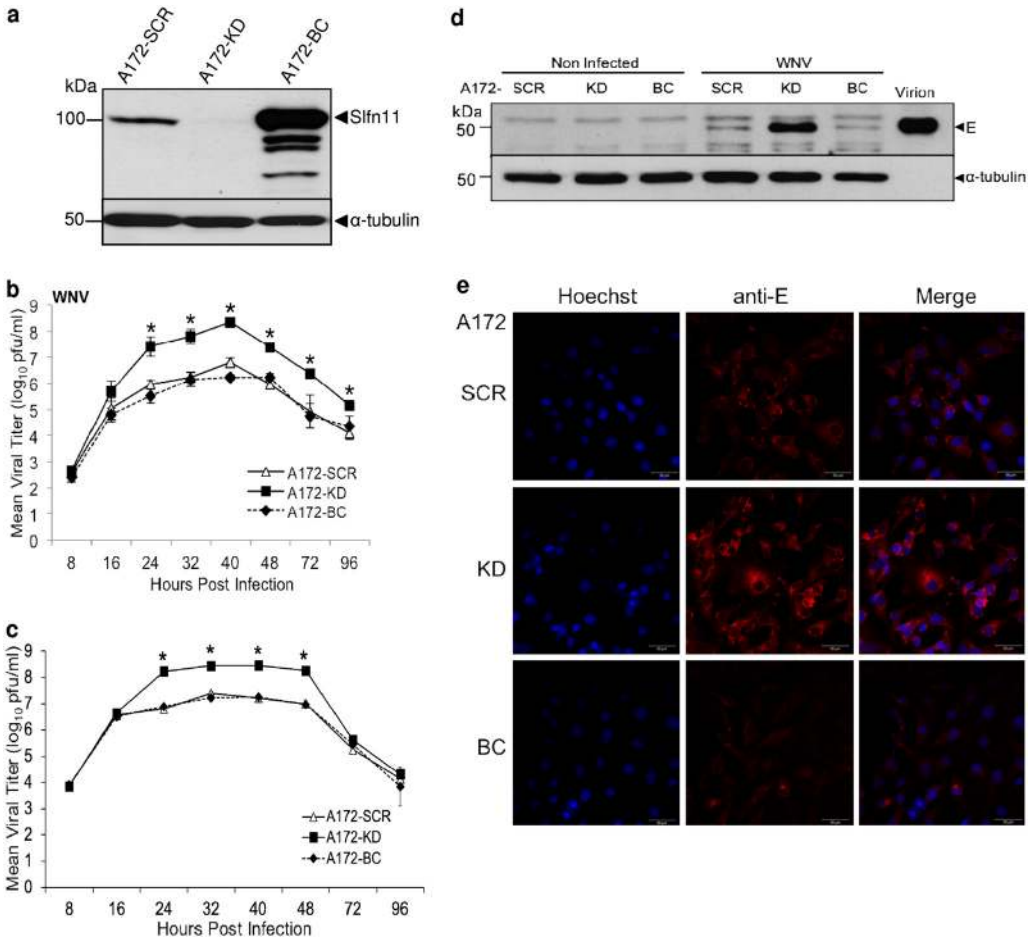

FIG 2 Effect of Slfn11 on WNV replication. (a) Immunoblot analysis of the expression of Slfn11 in A172 cells stably expressing shRNAs directed against Slfn11 (A172-KD) or scrambled (A172-SCR) RNA sequences and A172-KD cells engineered to reexpress Slfn11 (A172-BC). α-Tubulin was detected as a loading control. (b and c) WNV replication in A172-derived cells. A172-SCR, A172-KD, and A172-BC cells were infected with WNV (MOI of 0.1 [b] and MOI of 1 [c]), and viral replication was determined by quantification of the viral titer in the cell supernatant at different hours postinfection by a plaque assay. Statistically significant differences were calculated with repeated-measures ANOVA and Tukey-Kramer *post hoc* tests, and they are indicated with asterisks. Mean values and standard deviations indicate the variability of the viral titer found in triplicate plaque assays of samples from 8 independent infection experiments performed on different days with different viral preparations. *x* axes are not to scale. (d) Expression of WNV E in cells infected at an MOI of 0.1, evaluated by immunoblotting 40 h after infection. α-Tubulin was detected as a loading control. These results are representative of data from 3 independent infections. (e) Expression of WNV E (red) as detected by indirect immunofluorescence analysis of cells infected at an MOI of 1 at 48 h postinfection. Nuclei were labeled with Hoechst dye (blue).

replication was monitored at different times postinfection by titration of the cell supernatant by a plaque assay. Data in Fig. 3a show statistically significant interactions (df = 8, $F = 24.4$, and $P < 0.0001$). Interestingly, although A172-SCR cells did not support replication of DENV (Fig. 3a), Slfn11-deficient A172 cells efficiently allowed DENV replication, producing 2-log-higher viral titers than A172-SCR cells at the peak of replication. DENV reached titers of 10^6 PFU/ml in A172-KD cells, with a replication kinetic similar to that of WNV. In these experiments, DENV replication peaked from 24 to 32 h postinfection and then decayed by 48 h due to cytopathic effects. As expected, reexpression of Slfn11 in A172-KD cells (A172-BC cells) fully removed the permissiveness of these cells, highlighting the specificity of the effect of Slfn11 on DENV replication. Similarly to A172-SCR cells, DENV did not multiply in A172-BC cells. Therefore, basal expression levels of Slfn11 significantly contribute to the restriction of DENV replication in A172 cells.

Slfn11 and Slfn13 impair HIV-1 infection through a similar mechanism (4, 7). However, Slfn13 fails to restrict ZIKV replication (7), and the effect of Slfn11 on this flavivirus

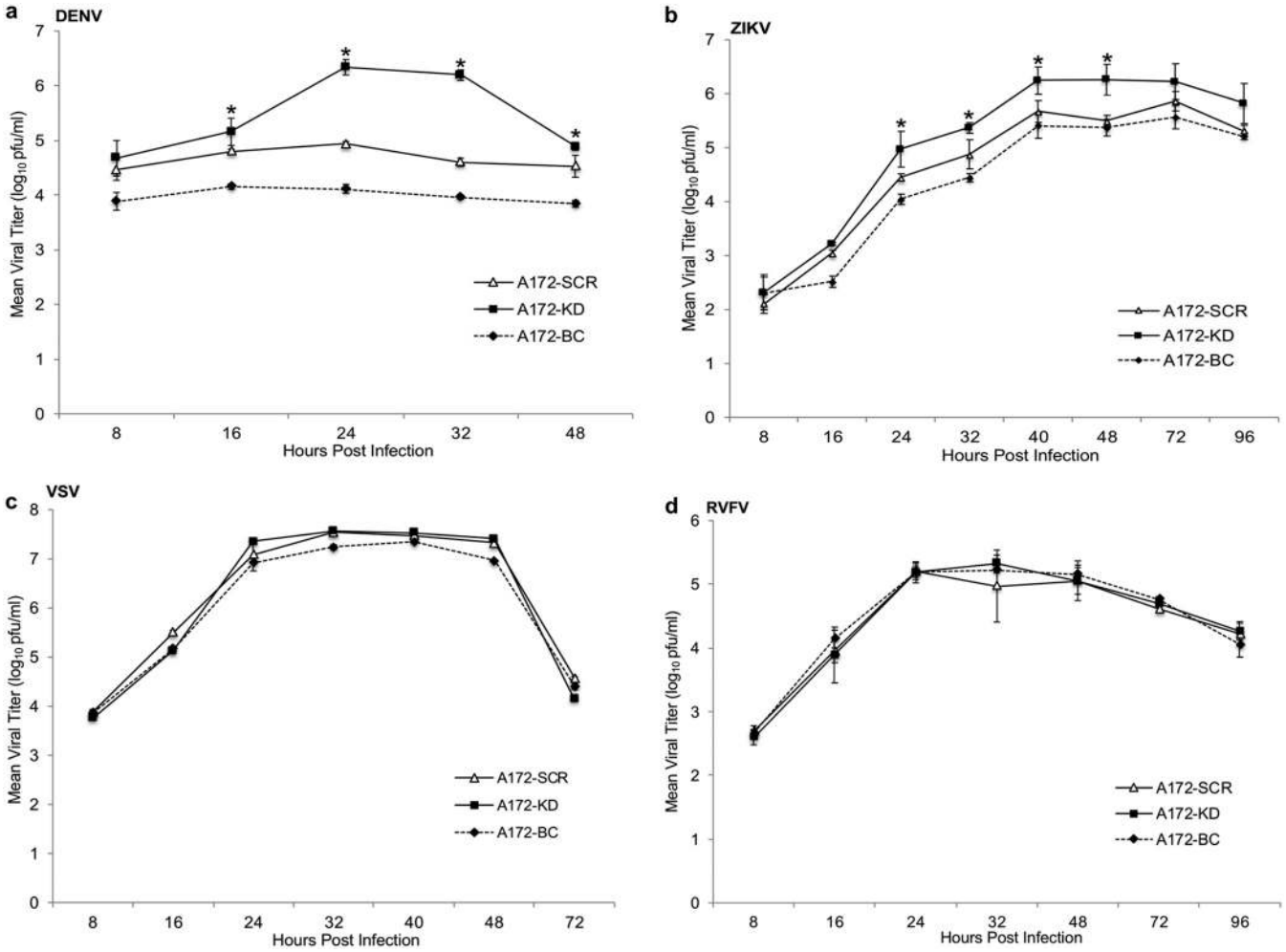

FIG 3 Effect of Slfn11 on viral replication. A172-SCR, A172-KD, and A172-BC cells were infected with dengue virus (DENV) (MOI of 0.1) (a), Zika virus (ZIKV) (MOI of 0.1) (b), vesicular stomatitis virus (VSV) (MOI of 0.1) (c), and Rift Valley fever virus (RVFV) (MOI of 0.1) (d). Viral replication was determined by quantification of the viral titer in the cell supernatant at different hours postinfection by a plaque assay. Statistically significant differences are indicated with asterisks and were calculated as described above. Mean values and standard deviations for each graphic represent the variability of the viral titer found in triplicate plaque assays of samples from 3 independent infection experiments performed on different days with different viral preparations. *x* axes are not to scale.

has not been explored yet. Thus, we determined whether or not Slfn11 impairs the replication of ZIKV. A172-derived cells were infected, and the ZIKV titer was quantified as described above. ZIKV replication peaked at 40 h postinfection and plateaued until 96 h postinfection or the end of the experiment. However, cytopathic effects were not very apparent even at these late time points of infection. Importantly, replication of ZIKV was also significantly enhanced by deficiency of Slfn11 (Fig. 3b), although the intensity of the effect was less marked than for WNV and DENV (df = 14, $F = 3.44$, and $P < 0.0009$). Nevertheless, a significant difference of an ~7-fold-higher titer was observed in A172-KD cells than in control cells from 24 to 48 h postinfection. Therefore, Slfn11 restricts ZIKV replication, in contrast to Slfn13 (7).

For comparison of patterns of (+)ssRNA and (−)ssRNA virus replication, we also tested the impact of Slfn11 knockdown and overexpression on the replication of the (−)ssRNA viruses VSV and RVFV MP12. The replication of both viruses was very robust in A172 cells, showing kinetics similar to that of WNV, with a peak of viral replication at 24 h postinfection (Fig. 3c and d). However, the replication of these (−)ssRNA viruses was very similar in terms of kinetics and titers among the different A172-derived cell lines evaluated, despite their differences in Slfn11 expression. Therefore, there was no

interaction between the effects of cell line on virus titer (df = 12, $F = 0.21$, and $P = 0.9963$ for VSV; df = 12, $F = 0.74$, and $P = 0.6974$ for RVFV).

The VSV used in these experiments is a recombinant virus expressing enhanced green fluorescent protein (eGFP) (11). Therefore, we also evaluated the titer of this virus obtained in the supernatants of the different A172-derived cell lines by flow cytometry analysis. A172-SCR and -KD cells were infected with VSV at three different MOIs (0.1, 0.3, and 1) in triplicates, and the viral supernatant was collected 24 h later. Next, SupT1 cells were infected with the viral supernatants and evaluated 24 h after infection by fluorescence-activated cell sorter (FACS) analysis. In agreement with the results of the plaque assays, we observed similar titers for the virus obtained from A172-SCR ($8.55 \times 10^4 \pm 0.84 \times 10^4$) and A172-KD ($8.58 \times 10^4 \pm 0.91 \times 10^4$) cells. In summary, data in Fig. 3c and d indicated that Slfn11 did not influence the replication of the (−)ssRNA viruses VSV and RVFV, highlighting the specificity of the antiviral activity of this protein for flaviviruses and lentiviruses (4).

From the results presented, it is also noteworthy that although A172-BC cells express markedly higher levels of Slfn11 than did A172-SCR cells (Fig. 2a), levels of replication of flaviviruses were similar in these two cell lines (Fig. 2b and c and Fig. 3a and b), suggesting that above certain levels, the antiviral effect of Slfn11 reaches saturation.

Mutagenesis analysis of Slfn11 antiviral activity. The N-terminal region of Slfn11 and Slfn13 harbors the anti-HIV-1 activity of these proteins (7). Not surprisingly, this region in both proteins contains the residues that in Slfn13 are responsible for the tRNA nucleolytic activity (7), which is central in the anti-HIV-1 activity of these proteins (12, 13). Therefore, we followed a previously described strategy (4) to determine whether the anti-WNV activity of Slfn11 also resides in the N-terminal region.

The N-terminal (amino acids 1 to 441) and the C-terminal (amino acids 442 to 901) regions of Slfn11 were expressed in A172-KD cells to generate the A172-N-term and A172-C-term cell lines (Fig. 4a), and their susceptibility to WNV was evaluated (Fig. 4b). Cells were infected with WNV at an MOI of 0.1, and viral replication was monitored by a plaque assay, as described above. WNV replication was impaired in cells expressing N-terminal Slfn11. Levels of viral replication were similar in these cells and in A172-BC cells that express full-length Slfn11. However, the level of WNV replication was significantly higher in cells expressing the Slfn11 C terminus (df = 14, $F = 11.69$, and $P < 0.0001$) (Fig. 4b). Therefore, these findings suggest a common antiviral mechanism of action of Slfn11 against HIV-1 (4) and WNV.

In order to define whether the subcellular distribution impacts the antiviral activity of Slfn11, we determined the localization of full-length Slfn11 and truncation mutants. A172-BC, -N-term, and -C-term cells were stained with anti-Slfn11 antibodies directed against the N terminus or the C terminus of the protein, and Slfn11 cellular distribution was determined by confocal microscopy analysis. Full-length Slfn11 accumulates in the nucleus, distributing homogenously in this organelle (Fig. 4c). However, both the C- and N-terminal Slfn11 proteins were uniformly distributed in the cytoplasm of the cell (Fig. 4c). The lack of an association of antiviral activity and the subcellular distribution of Slfn11 suggests that the process targeted by this protein is accessible in both the nucleus and the cytosol. In addition, these data confirm that the inactivity of the C-terminal region of Slfn11 is not determined by mislocalization or a gross defect in the intracellular solubility of this protein, for example, due to the formation of protein aggregates.

Effect of WNV infection and Slfn11 expression on the tRNA repertoire of A172 cells. It has been previously reported that Slfn11 counteracts the HIV-1-induced increase of the tRNA abundance, affecting viral protein expression (4). Importantly, pausing of translation elongation at codons recognized by low-abundance tRNAs might promote the efficiency of protein production and/or optimal protein folding (14–22). The latter mechanism enhances viral fitness (14, 15, 21). Therefore, we explored

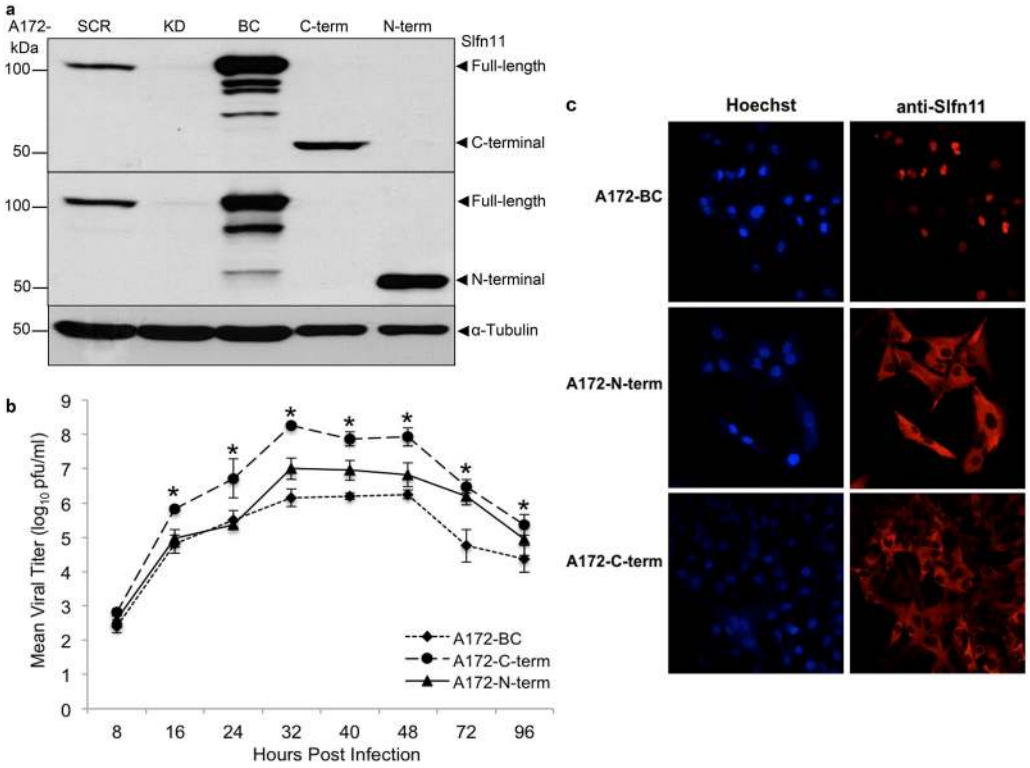

FIG 4 Mutagenesis analysis of antiviral activity of Slfn11. (a) Immunoblot analysis of the expression of Slfn11 in A172-derived cells. A172-KD cells were engineered to express the N or C terminus of Slfn11. A172-SCR, -KD, and -BC cells were used as controls. Different anti-Slfn11 antibodies were employed to identify the mutant proteins. α-Tubulin was detected as a loading control. (b) A172-BC, A172-N-term, and A172-C-term cells were infected with WNV (MOI of 0.1), and viral replication was determined by quantification of the viral titer in the cell supernatant at different hours postinfection. Statistically significant differences were calculated as described in the Fig. 2 legend and are indicated with asterisks. Mean values and standard deviations represent the variability of the viral titer found in triplicate plaque assays of samples from 3 independent infection experiments. The *x* axis is not to scale. (c) Cellular distribution of full-length Slfn11 and deletion mutants. A172-BC, A172-N-term, and A172-C-term cells were fixed/permeabilized and stained with the anti-Slfn11 antibodies used in panel a. Cell nuclei were identified with Hoechst staining (blue staining).

whether WNV infection also induces changes in the tRNA repertoire and whether these changes are opposed by Slfn11.

A172-SCR, -KD, and -BC cells were infected with WNV at an MOI of 1, and their tRNA repertoire was determined 8 h later by tRNA PCR array according to procedures previously described (4, 23). We chose these experimental conditions for several reasons. At this early time point of the life cycle, the virus is already replicating (Fig. 1a and Fig. 2b and c), and the different cell lines studied exhibited similar viral loads (Fig. 2b and c). Despite ongoing viral replication, no IFN-β was detected in these cultures at 8 h postinfection, which, in contrast, showed marked and similar levels of this cytokine at 48 h postinfection (Fig. 5a). Similar IFN-β production kinetics were observed at MOIs of 0.1 and 1 (Fig. 1c and Fig. 5a). Importantly, cellular levels of Slfn11 did not influence the magnitude and kinetics of type I IFN induction in response to WNV infection (Fig. 5a). Therefore, modifications in the tRNA pool at 8 h postinfection are likely be a direct consequence of the infection of these cells with similar amounts of virus in the absence of virally induced type I IFN.

It has been previously reported that Vero cells infected with WNV at an MOI of 1 exhibit apoptosis only later than 32 h postinfection (24). Thus, the cell viability of A172-derived cells infected with WNV at an MOI of 1 is expected to be preserved at 8 h postinfection. Furthermore, at 8 h postinfection, we expected WNV replication to be very sensitive to the efficiency of translation due to the low availability of translation-competent viral RNA molecules caused by the low rate of synthesis of viral RNA characteristic of the early life cycle (12).

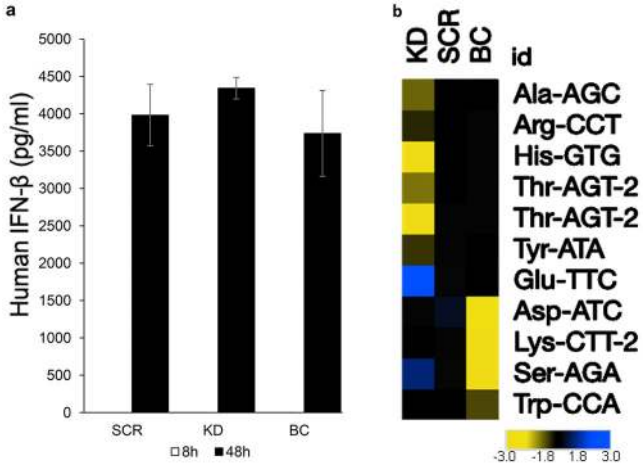

FIG 5 Effect of WNV infection on the tRNA pool of Slfn11-deficient and control cells. (a) Expression levels of IFN-β (all subtypes) in WNV-infected A172 cells. The culture supernatant was collected at 8 h and 48 h postinfection, and type I IFN was quantified by an ELISA. Data represent the means ± standard errors of the means from three independent infection experiments. (b) Heat map of fold changes of tRNAs up- or downregulated beyond the significance threshold. Each cell represents the tRNA ratio of infected/noninfected cells for each of the three cell lines evaluated. tRNAs that are increased (red cells), decreased (green cells), or unchanged (black cells) are indicated. The cutoff was set at a −1.89- to 1.89-fold change.

To ensure data robustness, the tRNA repertoire of infected and noninfected A172-derived cells was determined by using RNA obtained from three sets of independent experiments. tRNA levels were normalized to the levels of three housekeeping, noncoding RNAs (ncRNAs), all measured by real-time PCR in samples obtained from WNV-infected and noninfected cells (described in Materials and Methods). Next, the ratio of normalized tRNA levels in WNV-infected/noninfected cells was calculated and designated the WNV-induced tRNA fold change. For ratios of <1, the values were adjusted by dividing -1 by the ratio obtained to generate negative numbers. The WNV-induced tRNA fold change was determined for each of the 63 nuclear, amino-acid-coding tRNAs in the three A172-derived cell lines studied.

Analysis of the WNV-induced tRNA fold change indicated that only 11 of the 63 tRNAs evaluated varied past the threshold of significance that we established (±1.89-fold) in any of the cell lines studied. These findings indicated that WNV infection did not cause global modifications in the tRNA repertoire, in contrast to HIV-1 (4). Based on their WNV-induced fold change, the tRNAs in each of the three cell lines analyzed were classified as up- or downregulated when the fold change was positive or negative, respectively, regardless of whether they passed the significance threshold or not. Next, the average fold change (AFC) was calculated for each classification group and cell line. In A172-SCR cells, none of the tRNAs varied over the ±1.89-fold significance threshold in response to infection. The AFCs in these cells 1.46- and −1.22 for up- and downregulated tRNAs, respectively. Contrary to A172-SCR cells, which express physiological levels of Slfn11, WNV infection modulated tRNAs beyond the ±1.89-fold threshold in both Slfn11-deficient cells (A172-KD cells) and cells overexpressing this protein (A172-BC cells) (Fig. 5b and Table 1). In A172-KD cells, WNV infection significantly decreased the levels of six tRNAs, while the levels of two tRNAs increased, determining AFCs of −1.94 and 1.56, respectively. Note that the AFC of downregulated tRNAs passed the significance threshold (−1.89-fold). Importantly, seven of these eight tRNAs were not modified beyond the cutoff value in cells expressing Slfn11, suggesting that these virally induced changes were effectively counteracted by Slfn11. In contrast, the level of $tRNA^{Ser}AGA$, which was increased in A172-KD cells upon WNV infection, did not significantly change in A172-SCR cells, while in A172-BC cells, it was reduced past the significance threshold. In A172-BC cells, WNV infection significantly reduced the levels of three other tRNAs but did not upregulate any tRNA above the threshold (Fig. 5b and

TABLE 1 WNV-induced, Slfn11-specific tRNA changes[a]

Cell line	Amino acid	tRNA	Codon	Fold change in tRNA in infected/ noninfected cells	*P* value	Codon usage (%)
A172-KD	Ala	AGC	GCU	−2.11	0.0256	26.5
	Arg	CCT	AGG	−1.92	0.0136	14
	Glu	TTC	GAA	2.69	0.005	30.2
			GAG			31.5
	His	GTG	CAC	−8.63	0.0091	11.1
			CAU			7.5*
	Ser	AGA	UCU	2.11	0.0799	6.4
	Thr	AGT-2	ACU	−2.16	0.0082	15.3
	Thr	TGT-2	ACA	−9.8	0.0064	22.6
			ACG			11.8
	Tyr	ATA	UAU	−1.96	0.003	9.6*
A172-BC	Asp	ATC	GAU	−2.74	0.0422	21.5
	Lys	CTT-2	AAG	−3.30	0.0439	32
	Ser	AGA	UCU	−4.91	0.0283	6.4
	Trp	CCA	UGG	−2.02	0.0369	27

[a]Fold differences represent the ratios of tRNA in infected/noninfected A172-KD cells. WNV-induced tRNA changes in A172-BC cells are also included. Fold differences represent the ratios of tRNA in infected/noninfected A172-BC cells. The statistical significance of the changes in tRNA levels is represented by the calculated *P* values. The percentage of codons decoded by each tRNA in the WNV coding sequence is indicated. Rare codons for human usage are marked with an asterisk.

Table 1), yielding AFCs of −1.36 and 1.11, respectively. Although 93.6% of the tRNAs evaluated were similarly impacted by WNV infection in A172-SCR and -BC cells, the levels of these four tRNAs found to be significantly reduced in A172-BC cells were not importantly changed in A172-SCR cells (Fig. 5b). We speculate that Slfn11-mediated, WNV infection-triggered degradation of these four tRNAs requires levels of Slfn11 higher than those found in A172-SCR cells. In support of this interpretation, it has been reported that transient overexpression of Slfn11 preferentially degrades a subset of tRNAs (25), potentially impairing protein expression from cotransfected plasmids in an unspecific manner (3). Nevertheless, WNV replicated similarly in A172-SCR and -BC cells, indicating that changes in the abundances of these four tRNAs did not impact WNV replication.

The six tRNAs significantly and specifically downregulated in A172-KD cells decode 11.8% of the WNV polyprotein (Table 1); this seems contradictory considering the more robust viral replication observed in these cells. However, multiple lines of evidence (discussed below) indicate that a reduced availability of cognate tRNAs pauses translation at elongation, favoring protein production and/or optimal protein folding (13–15, 17–22). The latter mechanism enhances viral fitness (14, 15, 21). In order to evaluate this hypothesis, we determined the ratio of genome-containing particles to PFU in the supernatant of cells expressing or lacking Slfn11. Viral titers were determined as described above (Fig. 2b), and genome-containing viral particles were quantified by measuring the genome copy number in the cell supernatant by reverse transcription (RT)-PCR. RNA was isolated from viral supernatants harvested at 24 h postinfection (analyzed in Fig. 2b) and used for RT-PCR with WNV-specific primers. In these experiments (Table 2), we observed that viruses produced in Slfn11-deficient cells have 102.4-

TABLE 2 Genome-to-PFU ratios in A172-derived cells[a]

Cell line	PFU/ml	No. of genomes/ml	Genome/PFU ratio
A172-SCR	1.22×10^6	1.85×10^8	1.52×10^2
A172-KD	1.25×10^8	1.72×10^9	1.37×10^1
A172-BC	2.90×10^5	1.53×10^8	5.28×10^2

[a]Viral supernatants used for Fig. 2b were used to obtain the number of viral genomes per milliliter by RT-qPCR. Data show the mean genome/PFU ratios from three individual experiments. The coefficients of variation (CV) from the triplicate experiments in the A172-SCR, and -KD, and -BC cell lines were 0.148, 0.246, and 0.209, respectively.

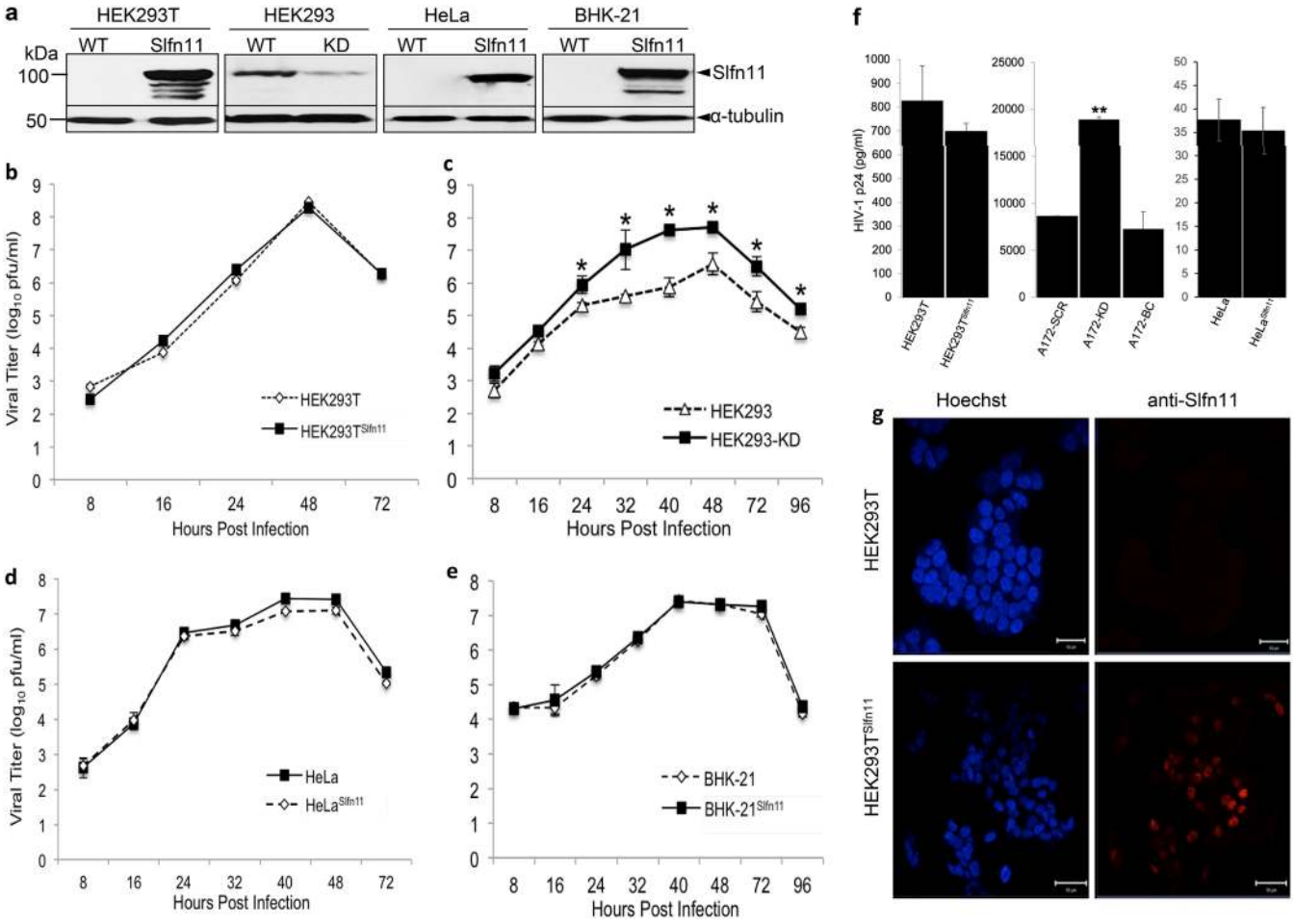

FIG 6 Evaluation of the antiviral activity of Slfn11 in HEK293T, HeLa, and BHK-21 cells. (a) Slfn11 expression in HEK293T, HEK293, HeLa, and BHK-21 parental and derived cell lines detected by immunoblot analysis. WT, wild type. (b to e) WNV replication in HEK293T^{Slfn11} (b), HEK293-KD (c), HeLa^{Slfn11} (d), BHK-21^{Slfn11} (e), and parental cell lines. Parental (open diamonds) and Slfn11-expressing derivative (filled triangles) cell lines as well as HEK293 and HEK293-KD cells were infected with WNV (MOI of 0.1), and viral replication was determined by quantification of the viral titer in the cell supernatant at different hours postinfection by a plaque assay. Statistically significant differences were calculated as described in the Fig. 2 legend and are indicated with asterisks. Mean values and standard deviations represent the variability of the viral titers found in triplicate plaque assays of samples from 3 independent infection experiments. (f) HIV-1 infection of cells expressing or not expressing Slfn11. Cells were infected with replication-defective HIV-1. Mean values and standard deviations represent the variability of HIV-1 p24 levels found in 3 independent infection experiments. Statistical analysis was performed by a *t* test (HEK293 and HeLa cells) and ANOVA with a Tukey honestly significant difference (HSD) *post hoc* test (A172). ** indicates a *P* value of <0.01. (g) Cellular distribution of Slfn11 in HEK293T^{Slfn11} cells. Cells were fixed/permeabilized and stained with an anti-Slfn11 antibody by indirect immunofluorescence (red). Nuclei were labeled with Hoechst dye (blue).

and 431-fold-higher PFU per milliliter than those obtained in A172-SCR and -BC cells, respectively. A172-KD cells also produced 9.3- and 11.2-fold more virions than A172-SCR and -BC cells, accounting for 11.1- and 38.5-fold-higher infectivities of A172-KD viruses than those produced in A172-SCR and -BC cells, respectively. These findings indicate that Slfn11 impairs the infectivity of the viral particles produced.

Lack of antiviral activity of Slfn11 in HEK293T, HeLa, and BHK-21 cells. Slfn11 has been shown to mediate antiviral activity in cells expressing endogenous Slfn11, such as CEM, HEK293 (3, 4), and A172 cells (Fig. 2b). However, the anti-WNV activity of this protein has not been evaluated in cells that naturally lack the expression of Slfn11 under basal conditions and/or following type I IFN stimulation (Fig. 1d). Among them, we characterized the WNV-permissive cell lines HEK293T, HeLa, and BHK-21 (baby hamster kidney fibroblasts). These cell lines were engineered to express Slfn11 (HEK293T^{Slfn11}, HeLa^{Slfn11}, and BHK-21^{Slfn11} cells) (Fig. 6a) and then used in viral infection experiments.

HEK293T-derived cells were infected with WNV at an MOI of 0.1, and viral replication was determined by a plaque assay as described above. WNV replicated robustly in these

cells (Fig. 6b), with kinetics similar to those of replication in A172 cells (Fig. 1a). However, WNV replication was indistinguishable between HEK293T cells expressing and those not expressing Slfn11 (Fig. 6b).

To further corroborate the lack of activity of Slfn11 in cells that do not naturally produce it, we evaluated the susceptibility of HEK293T and HEK293T^{Slfn11} cells to a single-round of infection with an HIV-1-derived reporter virus (Hluc). This virus expresses from the HIV-1 promoter a transcript that encodes viral proteins and the reporter protein firefly luciferase (26). Hluc infection was evaluated by measuring the level of the viral protein p24 in the cell supernatant by an ELISA and luciferase activity in cell lysates by using an enzymatic assay. HIV-1 p24 is produced by partial proteolysis from the viral precursor Gag. Importantly, both Gag and luciferase have poor codon adaptation indices, 0.68 and 0.66, respectively, and since Slfn11 has been reported to affect the expression of codon-biased open reading frames (3–5), we expected that HIV-1 p24 and luciferase levels would be affected by the expression of Slfn11 in HEK293T cells.

HEK293T and HEK293T^{Slfn11} cells were infected with Hluc, and luciferase activity and p24 levels were measured at 4 days postinfection. Intriguingly, we did not observe any significant effect of Slfn11 on luciferase activity. Cells expressing Slfn11 exhibited 1,740.4 $\pm$ 121 arbitrary units (AU)/ml, compared to parental cells that produced 1,188.4 $\pm$ 94.2 AU/ml. Furthermore, similar levels of HIV-1 p24 were also detected in these cells (Fig. 6f).

In contrast to HEK293T cells, the parental cell line HEK293 expresses endogenous Slfn11 and supports the anti-HIV-1 activity of this protein (4). Therefore, we determined the effect of Slfn11 on WNV replication in HEK293 cells. Control and Slfn11-deficient cells (Fig. 6a) were infected with WNV at an MOI of 0.1, and viral replication was monitored by a plaque assay as described above. WNV replication was very robust in HEK293 cells; however, Slfn11 knockdown significantly enhanced viral replication (df = 7, $F = 8.11$, and $P < 0.0001$) (Fig. 6c). These results demonstrated the anti-WNV activity of Slfn11 in HEK293 cells.

As an additional control, we evaluated the effect of Slfn11 on HIV-1 in A172-derived cells. A172-SCR, -KD, and -BC cells were infected with Hluc, and 4 days later, HIV-1 p24 and luciferase activities were measured. In contrast to HEK293T cells, the level of HIV-1 p24 expression was 2-fold higher in A172-KD cells than in A172-SCR and -BC cells (Fig. 6f). These results were in agreement with previously reported observations in CEM and HEK293 cells (4), indicating that Slfn11 restricts HIV-1 in A172 cells. Surprisingly, similar levels of luciferase activity were observed among the different cell lines evaluated. A172-SCR cells produced 1,072 $\pm$ 15 AU/ml, and A172-KD cells produced 1,227.5 $\pm$ 6.1 AU/ml, whereas A172-BC cells exhibited 1,289.4 $\pm$ 11.1 AU/ml of luciferase activity. These data indicate that Slfn11 levels did not affect the expression of a codon-biased, HIV-driven, nonviral protein.

We hypothesized that the absence of antiviral activity of Slfn11 in HEK293T cells could be due to a mislocalization of the exogenously expressed protein. Thus, we determined the subcellular distribution of Slfn11 in HEK293T^{Slfn11} cells by immunofluorescence analysis as described above. Similar to A172 cells (Fig. 4c), Slfn11 was localized entirely in the nucleus of HEK293T^{Slfn11} cells, and protein aggregates were not observed (Fig. 6g). Therefore, these findings exclude mislocalization or protein aggregation as a cause for the lack of activity of Slfn11 in HEK293T cells.

Next, we explored the effect of Slfn11 on WNV replication in HeLa and BHK-21 cells according to the procedures described above. HeLa and BHK-21 parental cells and cells engineered to express high levels of Slfn11 (HeLa^{Slfn11} and BHK-21^{Slfn11} cells) (Fig. 6a) were infected with WNV at an MOI of 0.1, and viral replication was monitored by a plaque assay. Similarly to HEK293T cells, replication of WNV in HeLa (Fig. 6d) and BHK-21 (Fig. 6e) cells was very robust and exhibited kinetics comparable to those of replication in A172 cells (Fig. 1a). However, in contrast to A172 cells, we did not find any differences in viral replication in HeLa or BHK-21 cells expressing Slfn11 or not (df = 6, $F = 2.42$, and $P = 0.0562$ for HeLa cells; df = 7, $F = 0.65$, and $P = 0.711$ for BHK-21 cells) (Fig. 6d and e).

Furthermore, we determined the effects of Slfn11 on single-round HIV-1 infection in HeLa cells as described above. Similarly to the above-described experiments, we did not observe differences in the luciferase levels in HeLa cells with or without Slfn11 expression. Parental cells expressed 18.73 ± 2.63 AU/ml, while cells engineered to express Slfn11 expressed 16.97 ± 1.59 AU/ml. Importantly, HIV-1 p24 levels were also similar in the HeLa cell lines (Fig. 6f), indicating that Slfn11 did not impair HIV-1 p24 production in HeLa cells. Therefore, our data indicated that HEK293T, BHK-21, and HeLa cells do not support the antiviral activity of exogenously expressed Slfn11. These results further support our hypothesis that Slfn11 is not the only component of this antiviral pathway.

DISCUSSION

Slfn11 and other members of this family, such as Slfn13 and Slfn14, have been shown to exhibit antiviral functions (4, 6, 7). In particular, Slfn11 impairs lentivirus infection, including HIV-1 (3, 4) and equine infectious anemia virus (5). This protein blocks HIV-1-induced upregulation of tRNA, a mechanism proposed to explain the deleterious effect of Slfn11 on viral protein expression (4). Slfn11 is absent in mice, and the ortholog of human Slfn11 in this species is unknown (1, 2), limiting the *in vivo* characterization of this protein.

The efficiency of protein translation is importantly influenced by tRNA availability; therefore, we postulated that Slfn11 would also selectively affect the replication of (+)ssRNA over (−)ssRNA viruses. In contrast to the latter group, (+)ssRNA viruses require the immediate translation of the incoming viral genome, making them more susceptible to impaired protein translation. Our data support these predictions. We found that Slfn11 severely affects the replication of flaviviruses, including WNV, DENV, and ZIKV; however, the (−)ssRNA viruses VSV and RVFV were not affected. The role of Slfn11 in the replication of other (+)ssRNA viruses deserves investigation. For example, infection of primary human monocyte-derived dendritic cells with the (+)ssRNA virus rhinovirus was reported to increase Slfn11 mRNA levels (27). These findings also indicate that cells that are relevant for flavivirus infection *in vivo* regulate Slfn11 expression in response to viral infection.

Notably, DENV was more susceptible to the effect of Slfn11 than the other viruses affected by this mechanism. Despite the fact that Slfn11 significantly impaired WNV, ZIKV, and HIV-1, these viruses successfully replicated in Slfn11-expressing cells. In contrast, DENV marginally replicated in cells expressing endogenous levels of Slfn11, and replication was further decreased in cells overexpressing the host protein. These data suggest that DENV could lack an anti-Slfn11 viral mechanism that is potentially present in WNV, ZIKV, and HIV-1.

Mechanistically, Slfn11 impairs WNV infectivity. Using reverse transcription-quantitative PCR (RT-qPCR) of virion-associated RNA, we found that although the titer of WNV produced in Slfn11-deficient cells was between 100- and 400-fold higher than the titers of viruses produced in cells expressing Slfn11, genome-containing particles were only 9- to 11-fold more abundant in the Slfn11-deficient cells. These findings strongly suggest that Slfn11 impairs WNV infectivity.

Our findings also revealed important differences between Slfn11 and Slfn13 regarding their specificity. Slfn13 failed to affect ZIKV replication (7), whereas Slfn11 is effective against this virus. These functional differences highlight the lack of redundancy in the antiviral specificity of different members of the Slfn family. Interestingly, placenta and testes, which are tissues potentially implicated in mother-to-fetus and sex-related transmission of ZIKV (28–30), lack expression of Slfn11, otherwise a ubiquitously expressed protein (3).

Combined analysis of our results and data previously reported (4) suggests some similarities as well as differences in the mechanism of action of this protein against flaviviruses and lentiviruses. In both cases, this protein blocks virus-induced changes in the tRNA repertoire of infected cells, and the N-terminal region of Slfn11 is necessary and sufficient for the antiviral activity. However, HIV-1 globally increased tRNA levels in

the absence of Slfn11 (4), in contrast to WNV infection, which modified only a subset of tRNAs in Slfn11-deficient cells.

Apparently, lentiviruses and flaviviruses have evolved different strategies to enhance viral replication by modulating the tRNA pool; however, the mechanism is still unknown. Lentivirus increases tRNA levels in the cell, resulting in a higher availability of tRNAs required for the translation of their codon-biased genome. In contrast, flaviviruses, which lack codon-biased genomes, diminish the abundance of only a subset of tRNAs. This selective effect of WNV on only a subset of tRNAs highlights their differential susceptibility to these virally exploited regulatory mechanisms. In support of this view, enzymes catalyzing tRNA posttranscriptional modifications, processing, and degradation, which importantly impact tRNA abundance, exhibit tRNA preferences (25, 31–37).

Predictably, the effects of WNV on the tRNA pool in the absence of Slfn11 will reduce the efficiency of viral protein translation; however, virus replication is markedly enhanced under these conditions. Multiple lines of evidence indicate that pausing of translation elongation at codons recognized by low-abundance tRNAs might promote the efficiency of protein production and/or optimal protein folding (14–22). A common pattern of 30 to 50 rare codons clustering immediately downstream of the start codon is present in highly expressed prokaryotic and eukaryotic genes. It is thought that this "ramp" sequence increases protein synthesis efficiency by reducing ribosome stalling during translational elongation (19). However, it is unlikely that the WNV-induced tRNA decrease will enhance viral replication by this mechanism, as the codons affected do not cluster in the viral genome.

Furthermore, it has been proposed that rare codons decrease the speed of translational elongation, potentially facilitating protein folding (16). In the RNA replicase and 3C protease of foot-and-mouth disease virus (15, 21) and in a *Neurospora crassa* circadian clock protein, a link between the location of rare codons and protein secondary structures was described (22). This link was also predicted by bioinformatics analysis of *Escherichia coli*, *Saccharomyces cerevisiae*, *Caenorhabditis elegans*, and *Drosophila melanogaster* genomes (22). The location of these codons in the transition boundaries of protein secondary structures suggests that the modulation of the speed of translation elongation is necessary for proper protein folding (16). Furthermore, replacement of native rare codons by synonymous common codons in the capsid of poliovirus (38) and hepatitis A virus (14) caused a decrease in viral fitness, suggesting that optimal protein folding due to a low abundance of tRNA results in increased viral fitness. Therefore, we postulate that the WNV-induced reduction in tRNA abundance in Slfn11-deficient cells leads to optimal viral protein folding and enhanced viral infectivity.

The relevance of Slfn11 in flavivirus replication adds further support to the role of tRNA function in the life cycle of these viruses. The expression of several aminoacyl-tRNA synthetases was upregulated at the protein or mRNA level in Vero cells or mouse brain upon infection with WNV or WNV and Japanese encephalitis virus, respectively (39). Importantly, changes in aminoacyl-tRNA synthetases observed in the mouse brain were flavivirus specific since reovirus infection did not modify their expression, even though infection by all three viruses upregulated the expression of 216 genes (39).

Considering the lack of response of the (−)ssRNA viruses VSV and RVFV to Slfn11, we propose that this type of virus does not alter the abundance of the tRNA pool. However, we lack evidence to support this hypothesis because the effect of viral infection on the host tRNA composition is ill defined. Nevertheless, it was demonstrated that influenza virus does not change the abundance of the tRNA repertoire (40), lending support to our hypothesis.

Intriguingly, we observed that exogenously expressed Slfn11 is not functional against HIV-1 or WNV infection in HEK293T, HeLa, and BHK-21 cells that naturally lack endogenous production of this protein. These observations suggest that Slfn11 is not the only component of this broad antiviral pathway. Furthermore, they indicate that the inhibitory effects of transiently expressed Slfn11 on the expression of transiently cotransfected plasmids, previously reported in HEK293T cells (3), do not mediate the antiviral activity of Slfn11.

We also observed a lack of correlation between the levels of Slfn11 and the antiviral effect of this protein. Slfn11 affected HIV-1 and flavivirus infection in A172-SCR and -BC cells to similar extents, although these cells express markedly different levels of Slfn11. These observations indicate that above certain levels of Slfn11, the antiviral activity of this protein reaches saturation.

The proposed role of Slfn11 in maintaining the stability of the tRNA pool could also explain the direct correlation between the sensitivity of cells to genotoxic drugs and their Slfn11 levels. It has been found that cancer cells expressing higher levels of Slfn11 are more sensitive to DNA-damaging agents (41–45). Thus, it is possible that higher levels of Slfn11 could reduce the abundance of specific tRNAs affecting the translation of DNA repair proteins encoded by codon-biased open reading frames (46).

In summary, our data indicate that Slfn11 opposes virus-induced changes in the tRNA repertoire, thus affecting evolutionarily unrelated viruses that manipulate the host tRNA repertoire to facilitate viral replication.

MATERIALS AND METHODS

Cell and virus culture. HEK293T, HeLa, SupT1, LLC-MK2, BHK-21, and A172 cells were obtained from the American Type Culture Collection (Manassas, VA). HEK293T, HeLa, BHK-21, and A172 cells were maintained in Dulbecco's modified Eagle's medium (DMEM); LLC-MK2 and BHK-21 cells were maintained in Eagle's minimum essential medium (E-MEM); and SupT1 cells were maintained in RPMI 1640. These culture media were supplemented with 10% fetal bovine serum (FBS), 1% penicillin and streptomycin, 1% nonessential amino acids (NEAA), and 1% sodium pyruvate. Maintenance medium used to perform viral infections consisted of E-MEM with L-glutamine, supplemented with 2% FBS, 1% NEAA, 1% sodium pyruvate, and 1% penicillin and streptomycin.

WNV strain TVP-7767 (passage 3 in Vero cells), RVFV strain MP-12 (passage 3 in Vero cells), and ZIKV strain MR-766 (passage 150 in suckling mouse brain and passage 3 in Vero cells) were obtained from the World Reference Center for Emerging Viruses and Arboviruses, University of Texas Medical Branch. DENV-2 strain 16681 (passage 9 in C6/36 cells) was obtained from Navy Medical Research Center 6. VSV engineered to express eGFP has been previously described (11). Viral stocks were prepared in Vero cells maintained in E-MEM supplemented with 2% FBS. The titer of each virus stock was determined via a plaque assay as described below.

A replication-defective HIV-1 reporter virus (Hluc) was used, which expresses long terminal repeat (LTR)-driven luciferase from the negative factor (NEF) slot and contains a large deletion in envelope (ENV) (26). Hluc was generated by calcium phosphate transfection of the corresponding HIV-1 expression plasmid (pHluc; 15 μg) and the VSV glycoprotein G (VSV-G)-encoding plasmid pMD.G (5 μg) into HEK293T cells, as described previously (26). In accordance with World Health Organization and Centers for Disease Control and Prevention guidelines, all work involving infectious WNV was performed in a biosafety level 3 (BSL-3) laboratory in accordance with biosafety practices described in the 2018 revised version of *The University of Texas at El Paso Biological Safety Manual* (47) and standard operating procedures. All work involving DENV, VSV, ZIKV, HIV-1, and RVFV MP-12 was performed in a BSL-2$^+$ laboratory in accordance with biosafety practices described in *The University of Texas at El Paso Biological Safety Manual*.

Virus replication dynamics. All cell lines infected with WNV, DENV, RVFV, ZIKV, and VSV were seeded in T25 cell culture flasks (2.5×10^5 cells in a 2-ml total volume) and allowed to grow overnight. The following day, the cells were infected with the respective viruses and incubated at 37°C for 1 h. Cells were subsequently washed three times with serum-free medium to remove input virus, replenished with maintenance medium, and incubated at 37°C. Cell culture supernatants were collected every 8 h until experiments were stopped and then stored at −80°C.

Plaque assay. Cell supernatants containing WNV or VSV were subjected to 10-fold serial dilutions, inoculated onto confluent monolayers of LLC-MK2 cells in 12-well cell culture plates, and incubated at 37°C for 1 h with gentle rocking every 15 min. The cells were then overlaid with 1 ml of 0.5% agarose in E-MEM maintenance medium. Cells were incubated at 37°C for 3 days and then stained with 1 g/liter of blue-black naphthol, 13.6 g/liter of anhydrous sodium acetate, and 60 ml/liter glacial acetic acid to visualize plaques. Plaque formation on each cell line was quantified, and viral titers were expressed as PFU per milliliter.

DENV titers were determined as previously described (48). Briefly, 3×10^5 BHK-21 cells were seeded in 12-well cell culture plates and then infected with viral supernatants at 37°C for 3 h, followed by the addition of 1 ml of 3% carboxymethylcellulose overlay medium. Cells were cultured for 5 days, followed by staining and quantification as described above.

RVFV and ZIKV plaque assays were performed as described above for WNV but using Vero 76 cells. RVFV- and ZIKV-infected cells were cultured at 37°C for 4 or 5 days, respectively. Staining and quantification were performed as described above.

Plaque assays for calculating viral titers were conducted in triplicate experiments with samples derived from independent viral infections.

Immunoblotting. Full procedures for protein detection by immunoblotting have been described previously (49). Briefly, cellular lysates were obtained by lysing cells with 2× Laemmli buffer and boiling

for 10 min. Cell lysates were resolved by SDS-PAGE and transferred overnight onto polyvinylidene difluoride (PDVF) membranes at 100 mA at 4°C. Membranes were blocked in Tris-buffered saline (TBS) containing 10% milk for 1 h and then incubated with the corresponding primary antibody diluted in TBS–5% milk–0.05% Tween 20 (antibody dilution buffer). Full-length Slfn11 and the Slfn11 C-terminal mutant were detected with anti-Slfn11 antibody E-4 (Santa Cruz Biotechnology) (1/500). The Slfn11 N-terminal mutant was detected with anti-Slfn11 antibody D-2 (Santa Cruz Biotechnology) (1/500). WNV envelope protein was detected with antibody PA1-41073 (Thermo Fisher Scientific) (1/500). Tetherin (BST-2) was detected with anti-BST-2 antibody (Santa Cruz Biotechnology) (1/500). α-Tubulin was detected as a loading control with antibody from clone B-5-1-2 (Sigma) (1/4,000). Membranes were incubated overnight at 4°C with primary antibodies, whereas anti-α-tubulin monoclonal antibody (MAb) was incubated for 30 min at 25°C. Primary antibody-bound membranes were washed in TBS–0.1% Tween 20, and bound antibodies were detected with goat anti-mouse IgG-horseradish peroxidase (HRP) (Sigma) (1/2,000) or goat anti-rabbit IgG-HRP (EMD Millipore) (1/4,000), followed by chemiluminescence detection. Densitometry of selected bands was quantified based on their relative intensities using Image Studio software (Li-Cor, Lincoln, NE).

Plasmids. For the generation of HIV-1-derived viral vectors, plasmids were obtained from the Eric Poeschla laboratory (Mayo Clinic, Rochester, MN) (49). These lentiviral vectors were used to express Slfn11 shRNA, control shRNA, and Slfn11 proteins. They were generated with packaging plasmid pCMVΔR8.91, a transfer plasmid derived from pTRIP (described below), and the envelope plasmid pMD.G encoding VSV-G.

(i) Slfn11 and SCR shRNA plasmids. An shRNA construct (top, 5′-GATCCGGCTCAGAATTTCCGTAC TGAATTCAAGAGATTCAGTACGGAAATTCTGAGCTTTTTTGGAAA-3′; bottom, 5′-AGCTTTTCCAAAAAAGCTC AGAATTTCCGTACTGAATCTCTTGAATTCAGTACGGAAATTCTGAGCCG-3′) against Slfn11 was designed using a target sequence that has been previously described (4). Briefly, the Slfn11 shRNA construct was ligated into the pSilencer 2.1 U6 Hygro shuttle vector (catalog number AM5760; Thermo Fisher Scientific), and the sequence was verified. Control shRNA contains a scrambled sequence (SCR) that was obtained from the negative-control plasmid provided with the kit. The Slfn11 and SCR shRNA expression cassettes were amplified by PCR and ligated into a unique PpUMI site in the HIV-1-derived transfer plasmid pTRIP-eGFP, and their sequences were verified.

(ii) shRNA-resistant Slfn11 expression plasmid. The shRNA-resistant Slfn11 cDNA was engineered by introducing 7 synonymous mutations within the 21-nucleotide (nt)-long shRNA target sequence of Slfn11. Plasmid pCDNA-V5-His-Slfn11 (Michael David, University of California—San Diego) (4) was used as the template for the Phusion high-fidelity DNA polymerase (catalog number F530S; Thermo Fisher). Primers used to introduce mutations were forward primer 5′-TCGGACCGAGGATGGGGACTGGTATGGG-3′ and reverse primer 5′-AAGTTTTGCGCTTCGTCAATGACG-3′. The newly created shRNA escape mutant cDNA was then amplified using the high-fidelity Deep Vent DNA polymerase (New England Biolabs), digested with SbfI and SpeI restriction enzymes, and cloned into unique SbfI-SpeI sites in the pTRIP-IRES-P HIV-1-derived transfer plasmid, and the sequence was verified.

(iii) N- and C-terminal Slfn11 mutant expression plasmids. The pTRIP-IRES-P-Slfn11-shRNA-resistant plasmid was used as the template to generate the Slfn11 truncated mutants using the QuikChange Lightning site-directed mutagenesis kit (Agilent Technologies). The mutant expressing N-terminal Slfn11 (amino acids 1 to 441) was generated with forward primer 5′-GAACAAAAACTCATCT CAGAAGAGGATCTG-3′ and reverse primer 5′-GAAGATCAAAATTCCCCGAAAGAAAG-3′, whereas forward primer 5′-TCTAGAAGTTGGGCTGTGGACC-3′ and reverse primer 5′-CATACTAGTGGATCCTCTAGC-3′ were used to produce C-terminal Slfn11 (amino acids 442 to 901). Mutants were verified by DNA sequencing.

Production of lentiviral vectors. The full procedures for transfection and production of lentiviral vectors have been described previously (26, 49, 50). Briefly, HEK293T cells were calcium-phosphate transfected with the corresponding transfer plasmid derived from pTRIP (15 μg), packaging plasmid pCMVΔR8.91 (15 μg), and VSV-G envelope expression plasmid pMD.G (5 μg). The viral supernatants were harvested at 48 h posttransfection and concentrated by ultracentrifugation at 124,750 $\times$ *g* for 2 h on a 20% sucrose cushion.

(i) Expression of Slfn11 and SCR shRNAs in A172 cells. A172 cells were transduced with shRNA- and eGFP-expressing lentiviral vectors, and cells expressing the highest 10% of eGFP fluorescence were isolated by cell sorting and expanded in culture. Slfn11 levels were determined in these cells by immunoblotting, as described above.

(ii) Expression of full-length Slfn11 and deletion mutants in Slfn11-deficient cell lines. A172-KD, HEK293T, BHK-21, and HeLa cells were engineered to express Slfn11 proteins by transduction with lentiviral vectors expressing Slfn11 and the puromycin resistance gene. Briefly, viral vectors were produced in HEK293T cells by transfection with the pTRIP-IRES-P-Slfn11-shRNA-resistant transfer plasmid expressing full-length Slfn11 or deletion mutants (15 μg) and the packaging and envelope expression plasmids described above. Viral supernatants were concentrated by ultracentrifugation and used to transduce cells. Three days later, transduced cells were selected in the presence of puromycin (3 μg/ml for A172-KD and HEK293T cells, 0.375 μg/ml for HeLa cells, and 6 μg/ml for BHK-21 cells). Slfn11 expression was verified by immunoblotting.

Single-round infectivity assay. HEK293T-, HeLa-, and A172-derived cells were seeded onto 24-well plates (2×10^4 cells/well) and allowed to grow overnight. The next day, cells were infected with Hluc, and 24 h later, the cells were extensively washed to remove the input virus. Four days later, the cell culture supernatant was collected for HIV-1 p24 quantification, and cell lysates were prepared in a buffer containing 1% Triton X-100 for luciferase activity quantification (Bright-Glow luciferase assay system; Promega), according to the manufacturer's instructions. Luciferase activity was determined in triplicate

samples using a microplate luminometer reader (Luminoskan Ascent; Thermo Scientific). Luciferase and HIV-1 p24 samples were derived from at least three independent infections.

HIV-1 p24, IFN-α, and IFN-β ELISAs. HIV-1 infection was measured by quantifying HIV-1 p24 in the supernatant of infected cells (described above) by an ELISA (catalog number 0801008; ZeptoMetrix Corporation). IFN-α and -β levels were quantified in the cell supernatants of infected cells by an ELISA (catalog numbers 41115-1 for IFN-α and 41415-1 for IFN-β; PBL Assay Science). ELISAs were performed according to the manufacturer's instructions.

Indirect immunofluorescence microscopy. Indirect immunofluorescence microscopy was used for determining WNV infection in A172-derived cells and for localizing Slfn11 in A172- and HEK293T-derived cells. A172-derived cells (1.5×10^4/well) were seeded onto 96-well confocal microscopy plates and infected with WNV at an MOI of 1 24 h later. Infected cells were fixed and permeabilized with Cytofix/Cytoperm buffer (catalog number 554714; BD Biosciences) at 24 h and 48 h postinfection and then stained with an anti-flavivirus group antigen monoclonal antibody that recognizes WNV envelope protein (clone D1-4G2-4-15; ATCC) (1/200) for 2 h at room temperature. Cells were then washed 3 times with phosphate-buffered saline (PBS) containing 0.1% FBS and then incubated with Alexa 568-conjugated antibody (10 μg/ml) (catalog number H-11004; Invitrogen) for 1 h at room temperature. Cells were again washed 3 times with PBS, and cell nuclei was stained with Hoechst 33342 (20 μg/ml) (catalog number H-3570; Invitrogen) for 10 min.

For subcellular localization of Slfn11, uninfected A172- and HEK293T-derived cells were staining as described above. Specifically, full-length Slfn11 and C-terminal mutants were detected with the anti-Slfn11 antibody E-4 (catalog number sc-374339; Santa Cruz Biotechnology) (1/200), and the Slfn11 N-terminal mutant was detected with anti-Slfn11 antibody D-2 (catalog number sc-515071; Santa Cruz Biotechnology) (1/200).

FACS infectivity assay. A172 and Vero cells were seeded onto 6-well plates (5×10^5 cells/well) and allowed to grow overnight. The next day, the cells were infected with WNV at an MOI of 1 and incubated at 37°C for 1 h. Cells were subsequently washed three times with serum-free medium to remove input virus, replenished with maintenance medium, and incubated at 37°C. At the indicated time points, cells were harvested, fixed, and permeabilized using Cytofix/Cytoperm buffer (catalog number 554714; BD Biosciences). Fixed cells were then stained with an anti-flavivirus group antigen monoclonal antibody that recognizes WNV E (clone D1-4G2-4-15; ATCC) (1/200) for 2 h at room temperature. Cells were then washed 3 times with 1× wash/permeabilization buffer and then incubated with Alexa 568-conjugated antibody (10 μg/ml) (catalog number H-11004; Invitrogen) for 1 h at room temperature. Cells were again washed 3 times with 1× wash/permeabilization buffer. The cells were then analyzed by flow cytometry using a Gallios flow cytometer (Beckman Coulter).

tRNA PCR array and analysis. To determine the effects of WNV infection on the host tRNA repertoire, we quantified the tRNA pool using a PCR-based methodology previously described (23). The procedure and data analysis were performed by Arraystar Inc. using the nrStar human tRNA repertoire PCR array. A172-derived cells were infected with WNV at an MOI of 1 for 1 h at 37°C, washed with fresh culture medium, and replenished with culture medium. At 8 h postinfection, cells were harvested, and total cellular RNA was extracted using TRIzol reagent. Experiments were performed in triplicate with appropriate noninfected controls. Total cellular RNA was sent to Arraystar Inc. for analysis. Briefly, quality control was performed on extracted RNA samples by using a NanoDrop ND-1000 instrument, and RNA integrity and genomic DNA contamination were assessed by denaturing agarose gel electrophoresis. Next, RNA samples were subjected to a demethylation step, followed by first-strand cDNA synthesis (rtStar tRNA-optimized first-strand cDNA synthesis kit, catalog number AS-FS-004; Arraystar). Real-time PCR was then performed using a proprietary human tRNA repertoire PCR array that is able to distinguish 66 nuclear tRNA isodecoders, covering all anticodons available in the GtRNAdb and tRNAdb databases. Three stably expressed small ncRNA genes, (i) RNU6-2, (ii) SNORD43, and (iii) SNORD95, were included in the array as the quantification references for tRNA and data normalization. One external RNA spike-in mix was added to the RNA sample prior to first-strand cDNA synthesis. The RNA spike-in control assay indicated the overall success and the efficiency of the reaction beginning from cDNA synthesis to the final qPCR. For the positive PCR control, two replicates of one artificial DNA and the PCR primer pairs were used to indicate the qPCR amplification efficiency. Only threshold cycle (C_T) values of >35 were considered good qPCR amplification efficiency and considered for analysis. The positive PCR control was used as an interplate calibrator and a control to exclude genomic DNA contamination.

RNA extraction. Total RNA was isolated from viral supernatants using TRIzol LS reagent (catalog number 10296010; Invitrogen) according to the manufacturer's instructions. All RNA samples had ratios of absorbance at 260/280 nm of 1.8 to 2.0, indicating that samples were contaminant-free. Purified RNA samples were stored at −80°C until used.

Quantification of WNV in cell culture supernatants. One-step RT-qPCR was carried out with the MiniOpticon real-time PCR system using the iTaq universal SYBR green one-step RT-PCR kit (catalog number 172-5151; Bio-Rad Laboratories, Hercules, CA, USA). After optimization, the reaction was performed in a final volume of 20 μl, including 10 μl 2× SYBR green RT-PCR mix, 0.6 μl (150 nM final concentration) of forward primer 5′-CCACCGGAAGTTGAGTAGACG-3′ and reverse primer 5′-TTTGCTAG CTTTAGGACCTACTATATCTACCTTTTGGTCACCCAGTCCTCCT-3′, 0.25 μl iScript reverse transcriptase, and 5 μl of the RNA template. These primers are specific to the 3′ untranslated region (UTR) of the WNV genome and have been previously described (51). The thermal cycling conditions consisted of a 10-min reverse transcription step at 50°C and 1 min of *Taq* at 95°C, followed by 45 cycles of PCR consisting of denaturing at 95°C for 10 s, annealing at 65°C for 30 s, and extension at 72.0°C for 90 s, with a single step of fluorescence emission data collection followed by a final extension step for 10 min at 72°C. The

specificity of the amplicon was verified by melting-curve analysis (55°C to 95°C), with a heating rate of 0.2°C per 5 s to verify the identity and purity of the amplified product. Triplicate reactions were carried out for each sample, and a no-template control was included. Cycling conditions and annealing temper atures were optimized using RNA purified from a WNV stock. Quantification was performed by constru cting a standard curve from serially diluted, known copy numbers of WNV genomes.

Bioinformatics analysis. Analysis of the impact of WNV-induced changes in tRNA on viral protein translation was performed by using a python script created to determine the differential tRNA expression values over the open reading frames within the viral genome. In short, the tRNA differential expression values were uploaded from the text file into a python dictionary. For each codon not found within the tRNA expression data set, the codon value was set to zero, and for redundant codons, it was limited to the highest expression value to limit the codon to a single value. Additionally, to make visualization of the values easier, a sliding-window approach was taken to average the differential expression over a desired number of amino acids. The window was then shifted by a consistent step size, and the average was again determined. To allow for variation in the resolution of the graphs, the window size and step size were coded as adjustable parameters within the python script for easy adjustment. For each gene, the individual codon usage and the windowed average values were written to a CSV file. The CSV file was then imported into Excel, and graphs were then created from the windowed codon usage.

Statistical analysis. All data used for viral replication curves were transformed to $\log_{10}$ PFU per milliliter. Repeated-measures ANOVA was used to test the impact of different cell lines expressing or not expressing Slfn11 on viral replication curves, and the Tukey-Kramer *post hoc* test was used to identify significant differences in viral titers between cell lines.

ACKNOWLEDGMENTS

This work was supported in part by a pilot project to M.L. and D.W. from grant number G12MD007592 from the National Institute of Minority Health and Health Disparities (NIMHD), National Institutes of Health (NIH). F.V. was supported by the Keelung Hong fellowship and by grant 5R25GM069621-11 (RISE program) from the National Institute of General Medical Sciences, NIH. We also thank the Biomolecule Analysis, Genomic Analysis, and Cytometry, Screening, and Imaging Core Facilities for technical help. These core facilities are supported by Research Centers in Minority Institutions program grant 5G12MD007592 from the NIMHD, NIH, to the Border Biomedical Research Center at The University of Texas at El Paso (UTEP).

We thank Zachary Martinez (UTEP) for help with HIV-1 p24 ELISAs and Michael David (University of California—San Diego) for providing us with an Slfn11 expression plasmid.

REFERENCES

1. Mavrommatis E, Fish EN, Platanias LC. 2013. The schlafen family of proteins and their regulation by interferons. J Interferon Cytokine Res 33:206–210. https://doi.org/10.1089/jir.2012.0133.
2. Schwarz DA, Katayama CD, Hedrick SM. 1998. Schlafen, a new family of growth regulatory genes that affect thymocyte development. Immunity 9:657–668. https://doi.org/10.1016/S1074-7613(00)80663-9.
3. Stabell AC, Hawkins J, Li M, Gao X, David M, Press WH, Sawyer SL. 2016. Non-human primate Schlafen11 inhibits production of both host and viral proteins. PLoS Pathog 12:e1006066. https://doi.org/10.1371/journal.ppat.1006066.
4. Li M, Kao E, Gao X, Sandig H, Limmer K, Pavon-Eternod M, Jones TE, Landry S, Pan T, Weitzman MD, David M. 2012. Codon-usage-based inhibition of HIV protein synthesis by human schlafen 11. Nature 491:125–128. https://doi.org/10.1038/nature11433.
5. Lin YZ, Sun LK, Zhu DT, Hu Z, Wang XF, Du C, Wang YH, Wang XJ, Zhou JH. 2016. Equine schlafen 11 restricts the production of equine infectious anemia virus via a codon usage-dependent mechanism. Virology 495:112–121. https://doi.org/10.1016/j.virol.2016.04.024.
6. Seong RK, Seo SW, Kim JA, Fletcher SJ, Morgan NV, Kumar M, Choi YK, Shin OS. 2017. Schlafen 14 (SLFN14) is a novel antiviral factor involved in the control of viral replication. Immunobiology 222:979–988. https://doi.org/10.1016/j.imbio.2017.07.002.
7. Yang JY, Deng XY, Li YS, Ma XC, Feng JX, Yu B, Chen Y, Luo YL, Wang X, Chen ML, Fang ZX, Zheng FX, Li YP, Zhong Q, Kang TB, Song LB, Xu RH, Zeng MS, Chen W, Zhang H, Xie W, Gao S. 2018. Structure of Schlafen13 reveals a new class of tRNA/rRNA-targeting RNase engaged in translational control. Nat Commun 9:1165. https://doi.org/10.1038/s41467-018-03544-x.
8. Schoggins JW, MacDuff DA, Imanaka N, Gainey MD, Shrestha B, Eitson JL, Mar KB, Richardson RB, Ratushny AV, Litvak V, Dabelic R, Manicassamy B, Aitchison JD, Aderem A, Elliott RM, Garcia-Sastre A, Racaniello V, Snijder EJ, Yokoyama WM, Diamond MS, Virgin HW, Rice CM. 2014. Pan-viral specificity of IFN-induced genes reveals new roles for cGAS in innate immunity. Nature 505:691–695. https://doi.org/10.1038/nature12862.
9. Valdez F, Salvador J, Palermo PM, Mohl JE, Hanley KA, Watts D, Llano M. 2018. Schlafen 11 restricts flavivirus replication. bioRxiv https://doi.org/10.1101/434563.
10. Koh WL, Ng ML. 2005. Molecular mechanisms of West Nile virus pathogenesis in brain cell. Emerg Infect Dis 11:629–632. https://doi.org/10.3201/eid1104.041076.
11. Stojdl DF, Lichty BD, tenOever BR, Paterson JM, Power AT, Knowles S, Marius R, Reynard J, Poliquin L, Atkins H, Brown EG, Durbin RK, Durbin JE, Hiscott J, Bell JC. 2003. VSV strains with defects in their ability to shutdown innate immunity are potent systemic anti-cancer agents. Cancer Cell 4:263–275. https://doi.org/10.1016/S1535-6108(03)00241-1.
12. Brinton MA. 2013. Replication cycle and molecular biology of the West Nile virus. Viruses 6:13–53. https://doi.org/10.3390/v6010013.
13. Goodman DB, Church GM, Kosuri S. 2013. Causes and effects of N-terminal codon bias in bacterial genes. Science 342:475–479. https://doi.org/10.1126/science.1241934.
14. Aragones L, Guix S, Ribes E, Bosch A, Pinto RM. 2010. Fine-tuning translation kinetics selection as the driving force of codon usage bias in the hepatitis A virus capsid. PLoS Pathog 6:e1000797. https://doi.org/10.1371/journal.ppat.1000797.
15. Ma XX, Feng YP, Liu JL, Ma B, Chen L, Zhao YQ, Guo PH, Guo JZ, Ma ZR, Zhang J. 2013. The effects of the codon usage and translation speed on protein folding of 3D(pol) of foot-and-mouth disease virus. Vet Res Commun 37:243–250. https://doi.org/10.1007/s11259-013-9564-z.

16. Pechmann S, Frydman J. 2013. Evolutionary conservation of codon optimality reveals hidden signatures of cotranslational folding. Nat Struct Mol Biol 20:237–243. https://doi.org/10.1038/nsmb.2466.
17. Quax TE, Claassens NJ, Soll D, van der Oost J. 2015. Codon bias as a means to fine-tune gene expression. Mol Cell 59:149–161. https://doi.org/10.1016/j.molcel.2015.05.035.
18. Rodrigue N, Philippe H, Lartillot N. 2010. Mutation-selection models of coding sequence evolution with site-heterogeneous amino acid fitness profiles. Proc Natl Acad Sci U S A 107:4629–4634. https://doi.org/10.1073/pnas.0910915107.
19. Tuller T, Carmi A, Vestsigian K, Navon S, Dorfan Y, Zaborske J, Pan T, Dahan O, Furman I, Pilpel Y. 2010. An evolutionarily conserved mechanism for controlling the efficiency of protein translation. Cell 141:344–354. https://doi.org/10.1016/j.cell.2010.03.031.
20. Zhao F, Yu CH, Liu Y. 2017. Codon usage regulates protein structure and function by affecting translation elongation speed in Drosophila cells. Nucleic Acids Res 45:8484–8492. https://doi.org/10.1093/nar/gkx501.
21. Zhou JH, You YN, Chen HT, Zhang J, Ma LN, Ding YZ, Pejsak Z, Liu YS. 2013. The effects of the synonymous codon usage and tRNA abundance on protein folding of the 3C protease of foot-and-mouth disease virus. Infect Genet Evol 16:270–274. https://doi.org/10.1016/j.meegid.2013.02.017.
22. Zhou M, Wang T, Fu J, Xiao G, Liu Y. 2015. Nonoptimal codon usage influences protein structure in intrinsically disordered regions. Mol Microbiol 97:974–987. https://doi.org/10.1111/mmi.13079.
23. Dittmar KA, Goodenbour JM, Pan T. 2006. Tissue-specific differences in human transfer RNA expression. PLoS Genet 2:e221. https://doi.org/10.1371/journal.pgen.0020221.
24. Chu JJ, Ng ML. 2003. The mechanism of cell death during West Nile virus infection is dependent on initial infectious dose. J Gen Virol 84:3305–3314. https://doi.org/10.1099/vir.0.19447-0.
25. Li M, Kao E, Malone D, Gao X, Wang JYJ, David M. 2018. DNA damage-induced cell death relies on SLFN11-dependent cleavage of distinct type II tRNAs. Nat Struct Mol Biol 25:1047–1058. https://doi.org/10.1038/s41594-018-0142-5.
26. Llano M, Saenz DT, Meehan A, Wongthida P, Peretz M, Walker WH, Teo W, Poeschla EM. 2006. An essential role for LEDGF/p75 in HIV integration. Science 314:461–464. https://doi.org/10.1126/science.1132319.
27. Puck A, Aigner R, Modak M, Cejka P, Blaas D, Stockl J. 2015. Expression and regulation of Schlafen (SLFN) family members in primary human monocytes, monocyte-derived dendritic cells and T cells. Results Immunol 5:23–32. https://doi.org/10.1016/j.rinim.2015.10.001.
28. Govero J, Esakky P, Scheaffer SM, Fernandez E, Drury A, Platt DJ, Gorman MJ, Richner JM, Caine EA, Salazar V, Moley KH, Diamond MS. 2016. Zika virus infection damages the testes in mice. Nature 540:438–442. https://doi.org/10.1038/nature20556.
29. Ma W, Li S, Ma S, Jia L, Zhang F, Zhang Y, Zhang J, Wong G, Zhang S, Lu X, Liu M, Yan J, Li W, Qin C, Han D, Qin C, Wang N, Li X, Gao GF. 2016. Zika virus causes testis damage and leads to male infertility in mice. Cell 167:1511.e10–1524.e10. https://doi.org/10.1016/j.cell.2016.11.016.
30. Rosenberg AZ, Yu W, Hill DA, Reyes CA, Schwartz DA. 2017. Placental pathology of Zika virus: viral infection of the placenta induces villous stromal macrophage (Hofbauer cell) proliferation and hyperplasia. Arch Pathol Lab Med 141:43–48. https://doi.org/10.5858/arpa.2016-0401-OA.
31. Elkordy A, Mishima E, Niizuma K, Akiyama Y, Fujimura M, Tominaga T, Abe T. 2018. Stress-induced tRNA cleavage and tiRNA generation in rat neuronal PC12 cells. J Neurochem 146:560–569. https://doi.org/10.1111/jnc.14321.
32. Fu H, Feng J, Liu Q, Sun F, Tie Y, Zhu J, Xing R, Sun Z, Zheng X. 2009. Stress induces tRNA cleavage by angiogenin in mammalian cells. FEBS Lett 583:437–442. https://doi.org/10.1016/j.febslet.2008.12.043.
33. Ivanov P, Emara MM, Villen J, Gygi SP, Anderson P. 2011. Angiogenin-induced tRNA fragments inhibit translation initiation. Mol Cell 43:613–623. https://doi.org/10.1016/j.molcel.2011.06.022.
34. Mesitov MV, Soldatov RA, Zaichenko DM, Malakho SG, Klementyeva TS, Sokolovskaya AA, Kubatiev AA, Mironov AA, Moskovtsev AA. 2017. Differential processing of small RNAs during endoplasmic reticulum stress. Sci Rep 7:46080. https://doi.org/10.1038/srep46080.
35. Thompson DM, Lu C, Green PJ, Parker R. 2008. tRNA cleavage is a conserved response to oxidative stress in eukaryotes. RNA 14:2095–2103. https://doi.org/10.1261/rna.1232808.
36. Torres AG, Batlle E, Ribas de Pouplana L. 2014. Role of tRNA modifications in human diseases. Trends Mol Med 20:306–314. https://doi.org/10.1016/j.molmed.2014.01.008.
37. Yamasaki S, Ivanov P, Hu GF, Anderson P. 2009. Angiogenin cleaves tRNA and promotes stress-induced translational repression. J Cell Biol 185:35–42. https://doi.org/10.1083/jcb.200811106.
38. Burns CC, Shaw J, Campagnoli R, Jorba J, Vincent A, Quay J, Kew O. 2006. Modulation of poliovirus replicative fitness in HeLa cells by deoptimization of synonymous codon usage in the capsid region. J Virol 80:3259–3272. https://doi.org/10.1128/JVI.80.7.3259-3272.2006.
39. Clarke P, Leser JS, Bowen RA, Tyler KL. 2014. Virus-induced transcriptional changes in the brain include the differential expression of genes associated with interferon, apoptosis, interleukin 17 receptor A, and glutamate signaling as well as flavivirus-specific upregulation of tRNA synthetases. mBio 5:e00902-14. https://doi.org/10.1128/mBio.00902-14.
40. Pavon-Eternod M, David A, Dittmar K, Berglund P, Pan T, Bennink JR, Yewdell JW. 2013. Vaccinia and influenza A viruses select rather than adjust tRNAs to optimize translation. Nucleic Acids Res 41:1914–1921. https://doi.org/10.1093/nar/gks986.
41. Barretina J, Caponigro G, Stransky N, Venkatesan K, Margolin AA, Kim S, Wilson CJ, Lehar J, Kryukov GV, Sonkin D, Reddy A, Liu M, Murray L, Berger MF, Monahan JE, Morais P, Meltzer J, Korejwa A, Jane-Valbuena J, Mapa FA, Thibault J, Bric-Furlong E, Raman P, Shipway A, Engels IH, Cheng J, Yu GK, Yu J, Aspesi P, Jr, de Silva M, Jagtap K, Jones MD, Wang L, Hatton C, Palescandolo E, Gupta S, Mahan S, Sougnez C, Onofrio RC, Liefeld T, MacConaill L, Winckler W, Reich M, Li N, Mesirov JP, Gabriel SB, Getz G, Ardlie K, Chan V, et al. 2012. The Cancer Cell Line Encyclopedia enables predictive modelling of anticancer drug sensitivity. Nature 483:603–607. https://doi.org/10.1038/nature11003.
42. Gardner EE, Lok BH, Schneeberger VE, Desmeules P, Miles LA, Arnold PK, Ni A, Khodos I, de Stanchina E, Nguyen T, Sage J, Campbell JE, Ribich S, Rekhtman N, Dowlati A, Massion PP, Rudin CM, Poirier JT. 2017. Chemosensitive relapse in small cell lung cancer proceeds through an EZH2-SLFN11 axis. Cancer Cell 31:286–299. https://doi.org/10.1016/j.ccell.2017.01.006.
43. Mu Y, Lou J, Srivastava M, Zhao B, Feng XH, Liu T, Chen J, Huang J. 2016. SLFN11 inhibits checkpoint maintenance and homologous recombination repair. EMBO Rep 17:94–109. https://doi.org/10.15252/embr.201540964.
44. Sousa FG, Matuo R, Tang SW, Rajapakse VN, Luna A, Sander C, Varma S, Simon PH, Doroshow JH, Reinhold WC, Pommier Y. 2015. Alterations of DNA repair genes in the NCI-60 cell lines and their predictive value for anticancer drug activity. DNA Repair 28:107–115. https://doi.org/10.1016/j.dnarep.2015.01.011.
45. Tang SW, Bilke S, Cao L, Murai J, Sousa FG, Yamade M, Rajapakse V, Varma S, Helman LJ, Khan J, Meltzer PS, Pommier Y. 2015. SLFN11 is a transcriptional target of EWS-FLI1 and a determinant of drug response in Ewing sarcoma. Clin Cancer Res 21:4184–4193. https://doi.org/10.1158/1078-0432.CCR-14-2112.
46. Goffena J, Lefcort F, Zhang Y, Lehrmann E, Chaverra M, Felig J, Walters J, Buksch R, Becker KG, George L. 2018. Elongator and codon bias regulate protein levels in mammalian peripheral neurons. Nat Commun 9:889. https://doi.org/10.1038/s41467-018-03221-z.
47. The University of Texas at El Paso. 2018. Biological safety manual. The University of Texas at El Paso, El Paso, TX. https://www.utep.edu/ehs/_Files/docs/manuals/Biosafety-Manual.pdf.
48. Morens DM, Halstead SB, Repik PM, Putvatana R, Raybourne N. 1985. Simplified plaque reduction neutralization assay for dengue viruses by semimicro methods in BHK-21 cells: comparison of the BHK suspension test with standard plaque reduction neutralization. J Clin Microbiol 22:250–254.
49. Garcia-Rivera JA, Bueno MT, Morales E, Kugelman JR, Rodriguez DF, Llano M. 2010. Implication of serine residues 271, 273, and 275 in the human immunodeficiency virus type 1 cofactor activity of lens epithelium-derived growth factor/p75. J Virol 84:740–752. https://doi.org/10.1128/JVI.01043-09.
50. Llano M, Gaznick N, Poeschla EM. 2009. Rapid, controlled and intensive lentiviral vector-based RNAi. Methods Mol Biol 485:257–270. https://doi.org/10.1007/978-1-59745-170-3_18.
51. Lim SM, Koraka P, Osterhaus AD, Martina BE. 2013. Development of a strand-specific real-time qRT-PCR for the accurate detection and quantitation of West Nile virus RNA. J Virol Methods 194:146–153. https://doi.org/10.1016/j.jviromet.2013.07.050.